On the occurrence and variability of the terdiurnal tide in the equatorial mesosphere and lower thermosphere and a comparison with the Kyushu-GCM

N. Venkateswara Rao,[1] T. Tsuda,[1] S. Gurubaran,[2] Y. Miyoshi,[3] and H. Fujiwara[4]

Received 25 May 2010; revised 1 October 2010; accepted 8 October 2010; published 27 January 2011.

[1] We studied the occurrence characteristics and variability of the terdiurnal tide (8 hour period) in the equatorial mesosphere and lower thermosphere (MLT), using a meteor radar at Koto Tabang (0.2°S, 100.3°E) and MF radars at Tirunelveli (8.7°N, 77.8°E) and Pameungpeuk (7.4°S, 107.4°E). These locations, one being located right over the equator and the other two at conjugate points around the equator within ±10°, form a unique experimental setup to study equatorial MLT dynamics. The terdiurnal tide exists as a distinct wave signature at all three locations. While the daily amplitudes can be as large as 15 m s^{-1}, the monthly mean amplitudes lie between 1 and 10 m s^{-1}. The amplitude of the terdiurnal tide at Pameungpeuk is generally smaller than that observed at Tirunelveli and Koto Tabang. The seasonal variation in amplitude shows both annual and semiannual oscillations of ~1 m s^{-1} at all three locations. The present observations combined with previous reports indicate that the timing of the primary maximum of the terdiurnal tide amplitude shifts from autumn to late spring and early summer as one moves from high latitudes to the equator (all with respect to the Northern Hemisphere). The amplitudes and seasonal variation in the present observations show good comparison with that simulated by the General Circulation Model (GCM) developed by Kyushu University, Japan. This study supports the occurrence of nonlinear interaction between diurnal and semidiurnal tides and shows that gravity waves play an important role in the generation of the terdiurnal tide.

Citation: Venkateswara Rao, N., T. Tsuda, S. Gurubaran, Y. Miyoshi, and H. Fujiwara (2011), On the occurrence and variability of the terdiurnal tide in the equatorial mesosphere and lower thermosphere and a comparison with the Kyushu-GCM, *J. Geophys. Res.*, *116*, D02117, doi:10.1029/2010JD014529.

1. Introduction

[2] Most of the observational records available up to now regarding tides in the Mesosphere and Lower Thermosphere (MLT) region extensively deal with diurnal (24 hour period) and semidiurnal (12 hour period) tides, which constitute the major part of MLT wind variability [*Manson and Meek*, 1986; *Vincent et al.*, 1998; *Tsuda et al.*, 1999; *Gurubaran et al.*, 2008]. In recent years, the scientific community dealing with MLT dynamics has well understood the significance of studying the terdiurnal tide (8 hour period) and its role in MLT wind variability and dynamics [*Teitelbaum et al.*, 1989; *Thayaparan*, 1997; *Jiang et al.*, 2009]. Being a third harmonic in the wind decomposition, its amplitude was often found to be less than that of simultaneously measured diurnal and semidiurnal tides. However, on many occasions the amplitude of the terdiurnal tide enhances so that it is comparable to that of diurnal and semidiurnal tides [*Cevolani and Bonelli*, 1985; *Reddi et al.*, 1993; *Thayaparan*, 1997; *Zhao et al.*, 2005].

[3] There have been many efforts to understand the detailed characteristics, variability, and global structure of the terdiurnal tide in the wind and temperature fields using data from MF and meteor radars [*Glass and Fellous*, 1975; *Teitelbaum et al.*, 1989; *Thayaparan*, 1997; *Younger et al.*, 2002; *Beldon et al.*, 2006], optical observations [*Pendleton et al.*, 2000], satellite observations [*Smith*, 2000], and theoretical simulations [*Teitelbaum et al.*, 1989; *Smith and Ortland*, 2001; *Akmaev*, 2001]. All of these studies report that the terdiurnal tide occurs as a distinct wave signature and shows clear seasonal variation.

[4] Seasonal variation in the terdiurnal tide amplitude has been studied with great interest since it can give us a clue in identifying the generation source of the terdiurnal tide and it helps us to quantify the contribution of the terdiurnal tide to MLT wind variability. The maximum amplitude of the terdiurnal tide occurs in different months at different latitudes. *Manson and Meek* [1986] reported that the amplitude attains

[1]Research Institute for Sustainable Humanosphere, Kyoto University, Uji, Japan.
[2]Equatorial Geophysical Research Laboratory, Indian Institute of Geomagnetism, Tirunelveli, India.
[3]Department of Earth and Planetary Sciences, Kyushu University, Fukuoka, Japan.
[4]Department of Geophysics, Tohoku University, Sendai, Japan.

0148-0227/11/2010JD014529

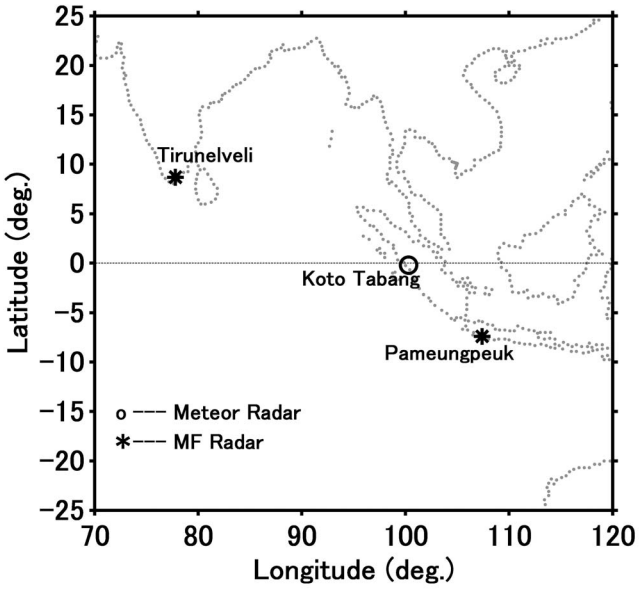

Figure 1. Map showing the location of the three radar sites used in the present study. The open circle and asterisks represent meteor radar and MF radars, respectively.

a maximum in winter (all seasons mentioned here are for the Northern Hemisphere) at Saskatoon (52°N, 107°W), with a secondary peak in July, which is more pronounced in the meridional wind. *Thayaparan* [1997] showed that large amplitudes of the terdiurnal tide occur at London, Canada (43°N, 81°W), with smaller amplitudes in summer and fall. *Younger et al*. [2002] reported a clear seasonal variation in the terdiurnal tide, with maximum amplitudes in late summer and autumn based on data from an all-sky VHF meteor radar at a high-latitude station at Esrange (68°N, 21°E). In a study performed at Castle Eaton, U. K. (52.6°N, 2.2°W), *Beldon et al*. [2006] found that the amplitudes are greatest in autumn and early winter (September-November), and the minimum occurs in early summer (May). In a recent study using a meteor radar at Maui, Hawaii (20.75°N, 156.43°W), *Jiang et al*. [2009] reported that at low latitudes the maximum amplitudes of the terdiurnal tide are seen during equinoxes, with a primary peak in March and a secondary peak in October. A similar result was obtained at a low-latitude Southern Hemisphere station at Cachoeira Paulista, Brazil (22.7°S, 45°W), where the maximum of the terdiurnal tide occurs during equinoxes (mainly during February-March) [*Batista et al.*, 2004; *Tokumoto et al.*, 2007]. Based on wind measurements by a High-Resolution Doppler Interferometer (HRDI) housed on the Upper Atmosphere Research Satellite (UARS), *Smith* [2000] found that the maximum amplitudes at midlatitudes occur during winter and fall equinox.

[5] The phase and vertical wavelength of the terdiurnal tide are found to vary widely as a function of season and latitude. They also differ between the zonal and meridional components. *Glass and Fellous* [1975] studied the terdiurnal tide from Garchy (47°N, 3°E) and found that the phase variations are irregular and that the vertical wavelengths are shorter in summer than in winter. *Manson and Meek* [1986] reported that the phase gradients are small in winter but large and irregular in summer. Likewise, *Cevolani* [1987], in a study from Budrio (45°N, 11.5°E) reported greater irregularity in phase variation during summer than in winter. *Younger et al*. [2002], on the other hand, have found that the vertical wavelengths at Esrange (68°N, 21°E) are shortest in winter and spring (25–35 km) and longest in summer and autumn (50–90 km). The phases vary during all months and show upward energy propagation. However, from a low-latitude location at Trivandrum (8.5°N, 77°E), *Reddi et al*. [1993] found a phase decrease with altitude during two June solstice months (1984 and 1987) and in November 1986, an increase in phase during December 1986, and a constant phase during January 1987. For a recent review of the terdiurnal tide see *Aso* [2003].

[6] Regarding the generation mechanism of the terdiurnal tide, three processes have been proposed: 1., Direct thermal excitation by solar heating [e.g., *Chapman and Lindzen*, 1970]; 2., nonlinear interaction between the diurnal and semidiurnal tides [*Glass and Fellous*, 1975; *Manson and Meek*, 1986; *Teitelbaum et al.*, 1989]; and 3., interaction of the diurnal tide with gravity waves [*Miyahara and Forbes*, 1991].

[7] Previous modeling studies on the terdiurnal tide have mainly considered the first two mechanisms and were able to account for the observed amplitude variations only during certain times of the year [*Teitelbaum et al.*, 1989; *Akmaev*, 2001]. However, no modeling study has considered the last mechanism in combination with the first two mechanisms. Thus, one reason for the discrepancies between observations and models could be that existing models do not consider all the sources that play an important role in the generation of the terdiurnal tide. Hence, it is important to assess the contribution of other sources such as gravity waves (GW). Another reason for the discrepancy could be the lack of a global view on the occurrence and variability of the terdiurnal tide. Although *Smith* [2000] examined global variability from satellite observations, the satellite measurement technique requires averaging for many days to obtain reliable amplitudes and to provide a global picture.

[8] Previous ground-based observations of the terdiurnal tide have been confined to latitudes higher than 20°, in both hemispheres. *Reddi and Ramkumar* [1997] and *Reddi et al*. [1993] studied the tide from Trivandrum, without attaining definitive conclusions on the seasonal variability. At this juncture, the study of terdiurnal tide from equatorial locations is very much essential to obtain a global picture of its occurrence and variability, and to understand the source mechanisms. The three radars used in the present study were chosen such that the Koto Tabang meteor radar is located at the equator (0.2°S) and the Tirunelveli and Pameungpeuk MF radars are at conjugate points within ±10° of the equator. These three locations provide a unique opportunity to determine the characteristics and variability of the terdiurnal tide in the equatorial MLT region and to obtain a latitudinal picture of its occurrence and variability.

2. Description of Radars and Data Analysis

[9] The MLT wind data used in this study were acquired using a meteor wind radar located at Koto Tabang (Indonesia; 0.2°S, 100.3°E) and MF radars located at Tirunelveli (India; 8.7°N, 77.8°E) and Pameungpeuk (Indonesia; 7.4°S, 107.4°E). The locations of the radars are shown in Figure 1 with the

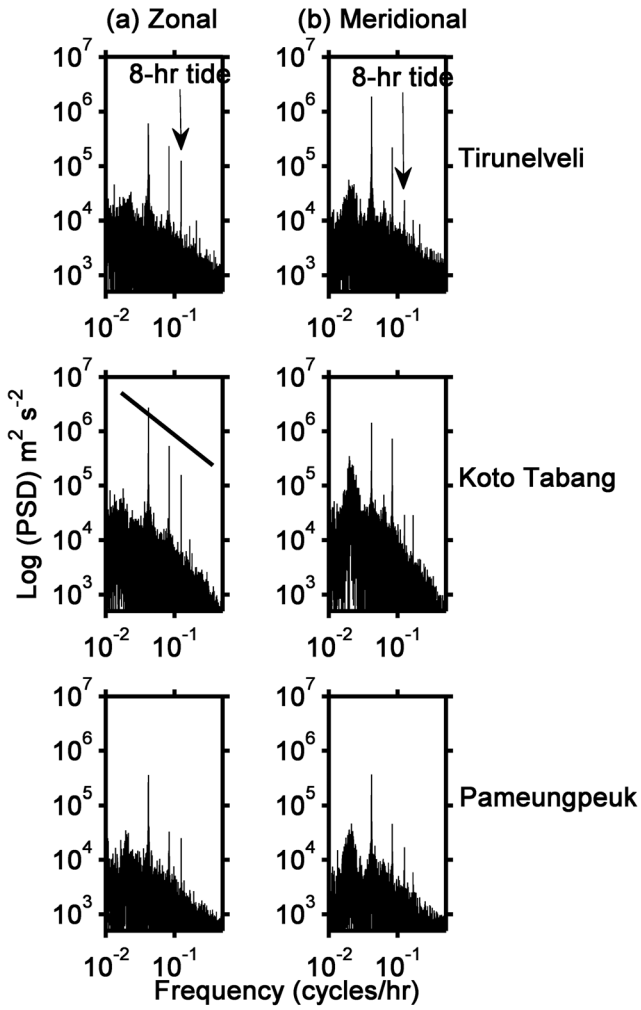

Figure 2. Logarithmic power spectral density of (a) zonal and (b) meridional winds observed at Tirunelveli (top), Koto Tabang (middle), and Pameungpeuk (bottom). The diagonal line in the middle panel in Figure 2a shows a slope of −5/3. Note that the presence of an 8 hour tide is indicated by an arrow in the top panels.

meteor radar being represented by a circle and the MF radars by stars.

[10] The MF radars at Tirunelveli and Pameungpeuk are operating at a frequency of 1.98 MHz and 2.008 MHz, respectively, and measure winds using the spaced antenna technique. These radars measure winds in the range of 78–98 km with resolutions of 2 km in height and 2 min in time. For both radars, the data acceptance rate is highest at ~88 km.

[11] The Koto Tabang radar is an all-sky interferometric meteor radar (SKiYMET; Mardoc and Genesis Software) and is operating at a frequency of 37.7 MHz with an output power of 12 kW. The interpulse period (IPP) is 400 ms, with a sampling pulse width of 13.3 ms (2 km range resolution). The typical meteor echo rate is between 3000 and 5000 d^{-1}, yielding estimates of horizontal wind velocity with time and altitude resolutions of 1 hr and 2 km, respectively.

[12] The Koto Tabang meteor radar provides hourly winds. The 2 minute wind observations from Tirunelveli and Pameungpeuk are averaged centering on each hour to obtain hourly mean winds. In the present study, we use these hourly winds from January 2003 to December 2007, between 78 and 98 km, to extract tidal parameters. Data from Tirunelveli and Koto Tabang are available for this period, although with some gaps. Major data gaps at Tirunelveli exist during 16–30 June 2003, 15 August to 11 September 2003, 18 August to 01 September 2004, and 26 September to 20 October 2006. At Koto Tabang, data gaps exist during 1–17 January 2003, 1 September to 1 October 2004, 14 April to 23 May 2004, and 25 September to 16 November 2005. The Pameungpeuk data start from 25 March 2004 and are available up to the end of 2006 with major gaps during 10 August 2004 to 6 November 2004, 7–28 July 2005, and 26 December 2006 to 13 January 2007. No data are available subsequent to 12 February 2007.

[13] The amplitudes and phases of diurnal, semidiurnal, terdiurnal, and quarter diurnal tides at the three locations are obtained by applying the least squares fitting method to the hourly wind data of zonal and meridional winds. In the present analysis, a 5 day data window, sliding forward by 1 day, is used for the extraction of tides. The 5 day window is chosen because, for the meteor radar at Koto Tabang, the meteor count is less during the daytime and requires sufficient averaging to obtain reliable winds for tidal fitting. The criterion used for the extraction of tidal parameters is that at least 16 hours (2/3 of a day) of data are available for each day in the 5 day window. The 5 day wind is then averaged at each time point to obtain the 24 hour composite wind. Each component of the wind can be expressed in terms of the prevailing wind and tidal components as

$$u(t) = u_0 + \sum_{k=1}^{4} u_k \cos\left(\frac{2\pi k}{T}(t - \varphi_k)\right), \quad (1)$$

where t is the local time, $u(t)$ is the wind data to be fitted, u_0 is the prevailing wind component, u_k and ϕ_k are the amplitude and phase of the respective tidal components (k = 1, 2, 3, and 4 correspond to the diurnal, semidiurnal, terdiurnal, and quarter diurnal components, respectively), and T = 24. The tidal parameters are individually estimated for zonal and meridional winds.

3. Results

3.1. Observation of the Terdiurnal Tide

[14] The presence of the terdiurnal tide with significant amplitudes and other tides is confirmed by subjecting the hourly zonal and meridional winds to a fast Fourier transform (FFT). The logarithmic power spectral density of zonal and meridional winds is shown in Figures 2a and 2b, respectively. The three panels in each of Figures 2a and 2b correspond to Tirunelveli (top), Koto Tabang (middle), and Pameungpeuk (bottom) radars. The line in the middle panel of Figure 2a represents the expected −5/3 slope due to the GW spectrum [*VanZandt*, 1982]. The power spectra at Tirunelveli and Pameungpeuk show nearly similar slopes (~−1.7), but the slope at Koto Tabang is much steeper (~−2.2). It is important to note that while the Tirunelveli and Pameungpeuk radars are MF radars, the Koto Tabang radar is a meteor radar. At all three locations, the presence of peaks with periods of 24 (diurnal tide), 12 (semidiurnal tide), and

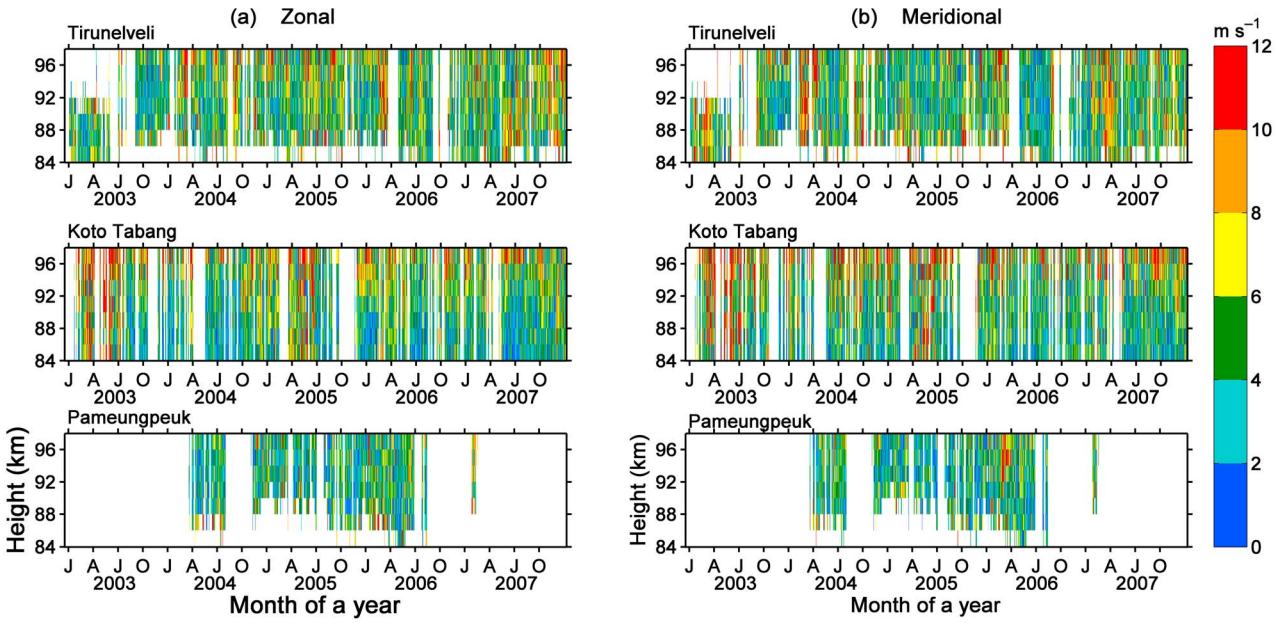

Figure 3. Height-time maps of the (a) zonal and (b) meridional components of the terdiurnal tidal amplitude observed at Tirunelveli (top), Koto Tabang (middle), and Pameungpeuk (bottom). The letters J, A, J, and O represent January, April, June, and October, respectively. White areas represent data gaps or a lack of sufficient data to estimate tidal amplitudes.

8 (terdiurnal tide) hours are clearly discerned above the background GW continuum. There is also a 6 hour tide, especially in the meridional wind. The diurnal tide is the dominant tidal component at all three locations, followed by the semidiurnal tide. The terdiurnal tide, which is the focus of the present study, is also present at all three locations; its amplitude is less than or comparable to that of the semidiurnal tide. The presence of the terdiurnal tide is indicated by a downward arrow in the uppermost panels of Figures 2a and 2b. Although the amplitude of the terdiurnal tide is less than that of the diurnal and semidiurnal tides, it has considerable amplitude and could influence the variability of MLT winds and dynamics.

[15] Gravity waves with similar periodicities to that of the terdiurnal tide can occur at the height of the MLT [*Younger et al.*, 2002] and may occasionally contribute to the observed 8 hour periodicity. Thus, before proceeding with the analysis, it is important to confirm that the observed 8 hour oscillation is not a manifestation of gravity waves. Because GW near the 8 hour period have random phases, they cannot produce a narrow peak in a spectrum calculated using a large data set (5 years), since the incoherent superposition of GW packets would self-cancel each other [i.e., *Younger et al.*, 2002]. Moreover the peak at 8 hours raises significantly above the GW background and suggests that the 8 hour periodicity is not due to gravity waves. Further, Lamb waves near 8 hour periodicity have been reported in the high-latitude MLT region [*Forbes et al.*, 1999]. However, even if such waves are present in the equatorial MLT region, they have short life times and hence cannot produce a peak calculated using a long data set [*Jiang et al.*, 2009]. Thus, it is unlikely that the 8 hour peak in the present observations originates from gravity waves or lamb waves; consequently it can be viewed as a manifestation of a tide.

3.2. Seasonal Variation in the Terdiurnal Tidal Amplitude

[16] To examine seasonal and interannual variabilities in terdiurnal tide amplitude, we plotted its zonal and meridional components in Figures 3a and 3b, respectively; as a function of month (from 2003 to 2007) and height. The three panels in Figures 3a and 3b correspond to amplitudes observed at Tirunelveli (top), Koto Tabang (middle), and Pameungpeuk (bottom). The amplitude of the terdiurnal tide seems to attain a maximum during equinoxes, especially during the spring equinox and early summer; these daily amplitudes reach a maximum of 15 m s^{-1}. This amplitude maximum, however, shows interannual variability. The zonal component of the terdiurnal tide shows little interannual variability, except that the Tirunelveli zonal component shows strong amplitudes during May-December 2007, larger than those in other years. The meridional component, however, shows strong interannual variability. At Tirunelveli, the amplitude enhancement is relatively prominent during 2003, 2004, and 2007. Little seasonal variability is seen during 2005, when the amplitude is relatively constant. At Koto Tabang, the amplitudes are stronger during April-June of 2003 and 2005 than during other years. For Pameungpeuk, the amplitudes are relatively strong during March-May 2006.

[17] To clearly show the seasonal variations, neglecting the interannual variability, we compiled the 5 year composite of monthly averaged terdiurnal tide amplitudes for zonal and meridional winds in Figures 4a and 4b, respectively. The criterion for calculating the monthly average is that at least 20 days of data are available in each month. To quantify the amount of seasonal variability, we fitted annual and semiannual oscillations (AO and SAO, respectively) to the monthly mean amplitudes, as shown on the right side of each panel in Figure 4. From Figure 4, the following

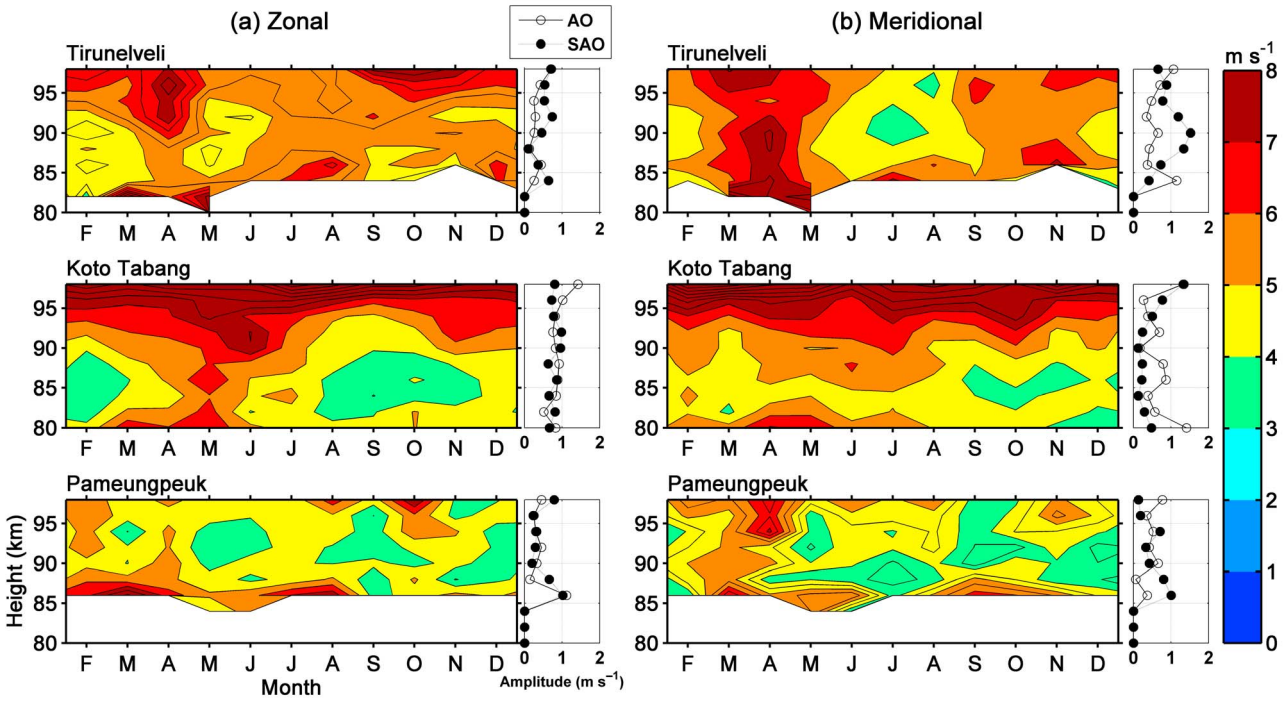

Figure 4. Height-month maps calculated using a 5 year composite of monthly mean amplitudes for the (a) zonal and (b) meridional components of the terdiurnal tide. The line plots to the right of each panel show amplitudes of annual (open circles; AO) and semiannual (closed circles; SAO) oscillations.

points can be noted: 1., The monthly mean amplitudes lie between 1 and 10 m s^{-1}; 2., the amplitudes at Pameungpeuk are always smaller than those observed at Tirunelveli or Koto Tabang, especially in the zonal wind (this feature is also apparent in Figure 3); 3., maximum amplitudes occur during March-May at Tirunelveli and Pameungpeuk and during April-June at Koto Tabang; and 4., the magnitudes of the AO and SAO are approximately equal in the zonal wind and have a maximum value of ~1 m s^{-1}. For the meridional component, SAO dominates AO at Tirunelveli and Pameungpeuk and whereas AO slightly dominates SAO at Koto Tabang.

3.3. Altitude Variation in Terdiurnal Tide Amplitude and Phase

[18] Figures 5a and 5b shows the altitude variation of the terdiurnal tide amplitude and phase for the zonal and meridional components, respectively. The four panels in each component represent the amplitudes and phases for the months of January, April, July, and October. The monthly mean amplitudes and phases were obtained by vector averaging [*Vincent et al.*, 1998]. The altitude variation of the terdiurnal tide amplitude at Koto Tabang shows that the amplitude decreases from 80 km up to 85–90 km, possibly due to dissipation of the tide, and then starts increasing gradually with increasing height due to decreasing air density. Amplitudes at the conjugate points of Tirunelveli and Pameungpeuk also decrease up to 85–90 km, again possibly due to dissipation of the tide; the subsequent increase at higher altitudes is less pronounced than that at Koto Tabang. This difference at higher altitudes could be due to the fact that a meteor radar is used at Koto Tabang whereas MF radars are used at the other two sites. Furthermore, the amplitudes at Pameungpeuk are generally smaller than those at Tirunelveli and Koto Tabang.

[19] In Figure 5 the altitude variation of the terdiurnal tide phase is shown on the right side of each panel. Here the phase is defined as the time when the maximum tidal amplitude was observed between 0000 and 0800 local time (LT). The altitude variation of the phase in both zonal and meridional winds at all three locations shows that the vertical wavelengths are large and that the tide is evanescent in character. If the tide is purely a migrating one, then the longitudinal differences among the three locations should result in tidal phase differences. Accordingly, when the phase is plotted in local time, as in Figure 5, the tidal phase at the three locations should be the same. However, the phase relationship between the three sites shows that the tide is not purely a migrating one and could be a mix of migrating and nonmigrating tides. Hence, it is difficult to directly estimate the vertical wavelengths. The phase difference between the zonal and meridional components varies with altitude.

3.4. Comparison with the Kyushu General Circulation Model

[20] In this section, we compare the terdiurnal tidal amplitudes observed at the three locations with output of a new General Circulation Model (GCM) developed by Kyushu University (Kyushu-GCM) [*Miyoshi and Fujiwara*, 2003]. This model is a global spectral model that contains the region from the ground surface to the exobase (500 km). The Kyushu-GCM solves the full nonlinear primitive equations for eastward and northward momentum, thermody-

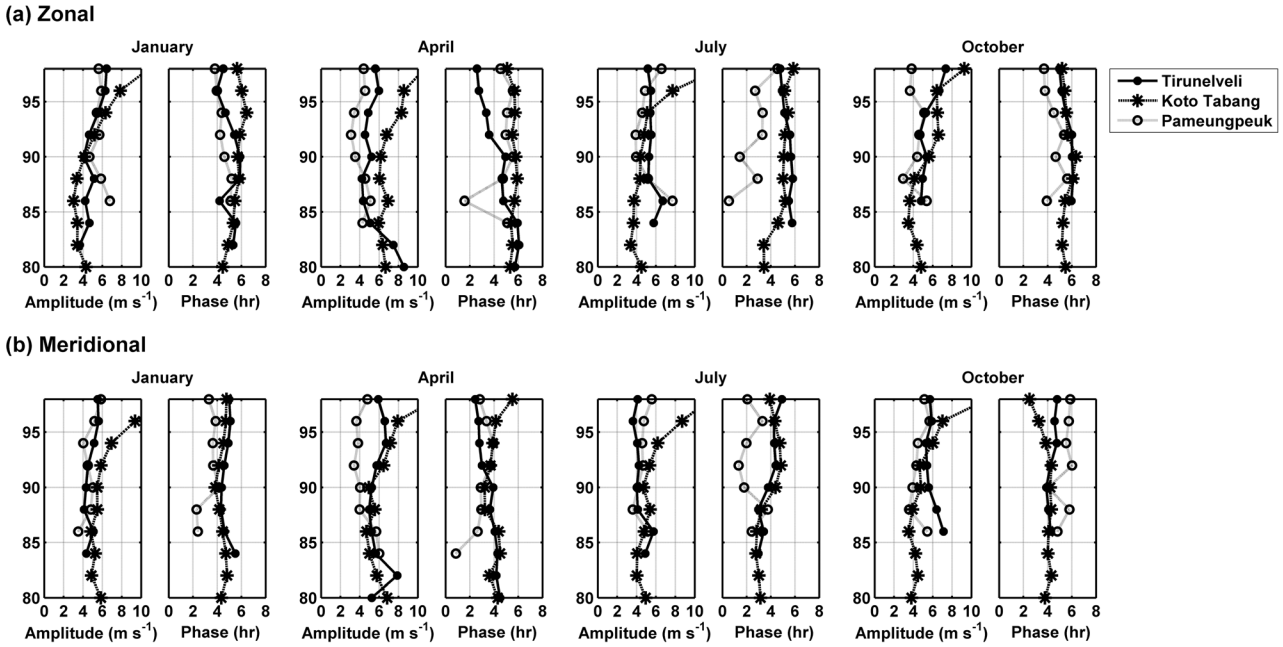

Figure 5. Height profiles of the terdiurnal tide amplitude and phase for the (a) zonal and (b) meridional components in January, April, July, and October. Closed circles, asterisks, and open circles represent data from Tirunelveli, Koto Tabang, and Pameungpeuk, respectively.

namics, continuity, and hydrostatics. It has a full set of the physical processes appropriate for the troposphere, stratosphere, mesosphere and thermosphere; thus, it includes both migrating and nonmigrating tides. Detailed descriptions of the physical processes that are included in the model can be found in *Miyahara et al*. [1993] and *Miyoshi* [1999].

[21] The amplitudes and phases of the terdiurnal tide from the Kyushu-GCM are extracted by subjecting the 5 day wind to least squares fitting (similar to the approach adopted in extracting the tides at the three locations) and shifting each time by 1 day. Figures 6a and 6b compare the observed terdiurnal tidal monthly mean amplitudes with that of Kyushu-

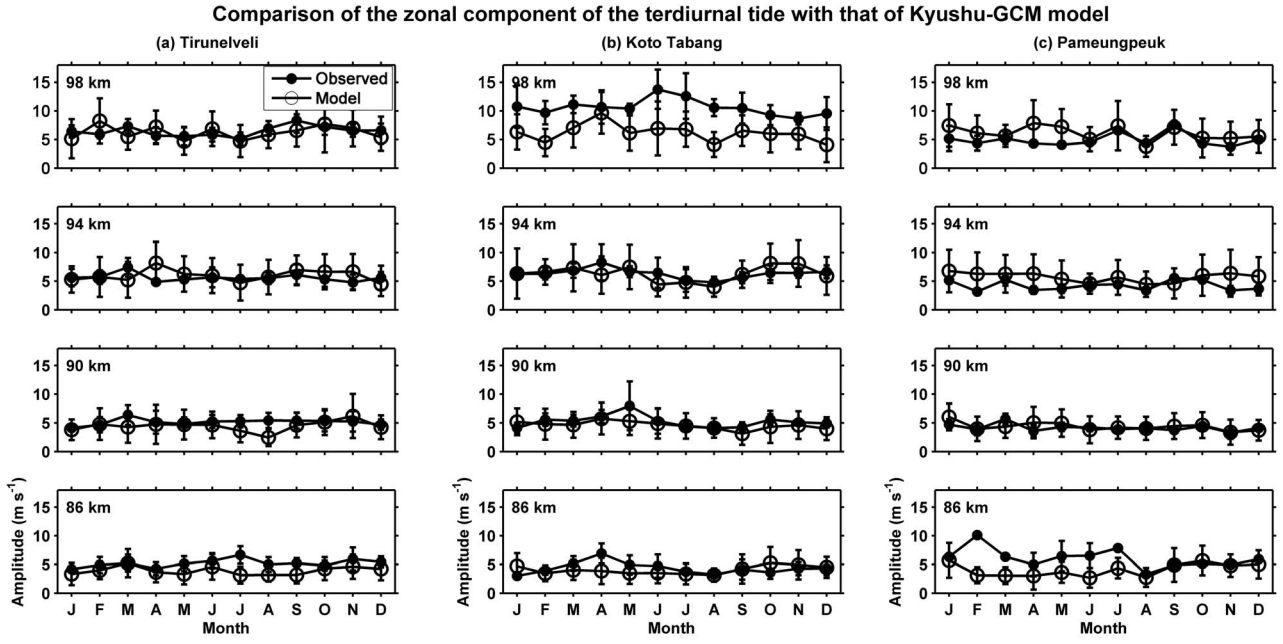

Figure 6a. The zonal component of the terdiurnal tide amplitude observed (closed circles) compared with values simulated by the Kyushu-GCM (open circles; Model) at (a) Tirunelveli, (b) Koto Tabang, and (c) Pameungpeuk for heights of (from top to bottom) 98, 94, 90, and 86 km.

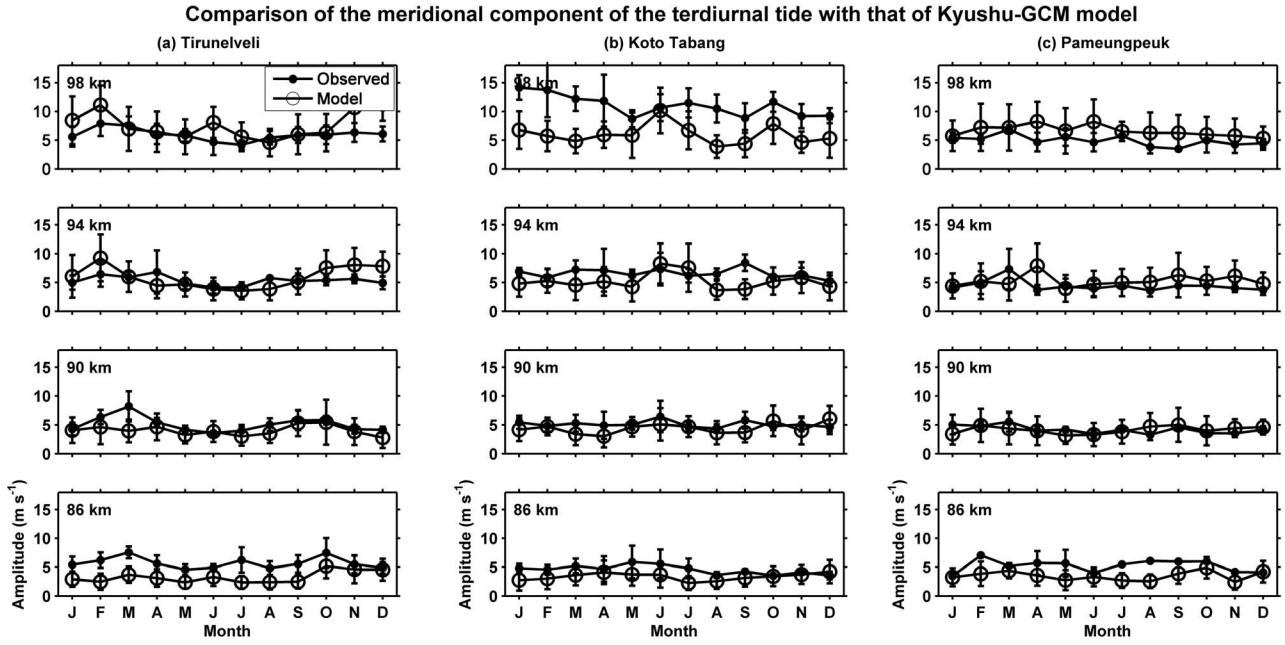

Figure 6b. As for Figure 6a, but for the meridional component.

GCM model for the zonal and meridional components, respectively. Comparisons of the modeled and observed tidal amplitudes for Tirunelveli, Koto Tabang, and Pameungpeuk are shown. The four panels for each location corresponds to heights of 98, 94, 90, and 86 km (from top to bottom).

[22] Figure 6a reveals that at Tirunelveli, the observed and modeled amplitudes are generally in good agreement. Observations exceed the model values during March at 98, 94, and 90 km, during August at 90 km, and during September at 98 km. At 86 km, the observed values exceed the model values throughout the year. At Koto Tabang (second column, Figure 6a) the observed values are generally in good agreement with the model values although the observed values exceed the model values during March-June at 86 km, during May at 90 km, and during April and June at 94 km. At 98 km, the observed amplitudes exceed the model values. At Pameungpeuk (third column, Figure 6a), however, the observed values are similar to or smaller than the model values at 90, 94, and 98 km. At 86 km, the observed values are greater than the model values during February-June and are similar to model values at other times. Thus there is some difference between the observed and modeled amplitudes, especially when the observed values are enhanced. The seasonal variation of the observed and modeled amplitudes, however, is nearly similar at all altitudes and locations.

[23] Figure 6b compares the observed and modeled meridional amplitudes. At Tirunelveli, the observed and modeled amplitudes show similar seasonal variations. At 86 km, the observed values are higher than the model values. At 90 km, the observed values agree well with the model results, except in March when the observed values show a sudden peak. At 94 and 98 km, the model values exceed the observed values, especially in winter months. At Koto Tabang (second column, Figure 6b), the observed amplitudes either exceed or are comparable to the model values. At Pameungpeuk (third column, Figure 6b), the observed values agree well with the model results, although at 86 km the observed values exceed the model results, and at 98 km the model values exceed the observations. Overall, the observed and modeled values show similar seasonal variations. Deviations are mainly seen when the observed values are enhanced.

4. Discussion

[24] We studied the terdiurnal tide variability in the MLT region at three equatorial locations using meteor radar observations from Koto Tabang and MF radar observations from Tirunelveli and Pameungpeuk. The salient features of our observations that require further discussion and comparison with other higher-latitude observations and models are: 1., large amplitudes of the terdiurnal tide in the equatorial region, with daily amplitudes as high as 15 m s^{-1} and monthly mean values between 1 and 10 m s^{-1}; 2., smaller amplitudes of the terdiurnal tide over Pameungpeuk than over Tirunelveli and Koto Tabang; and 3., seasonal variations in the amplitude of the terdiurnal tide with a maximum in March-May at Tirunelveli and Pameungpeuk and in April-June at Koto Tabang. We also examine and discuss the possible generation sources of the terdiurnal tide based on the present observations.

4.1. Comparison With Observations at Other Latitudes and With Model Results

[25] Previous studies on the terdiurnal tide at low, middle, and high latitudes showed that the terdiurnal tidal amplitude is generally less than that of the diurnal and semidiurnal tides, although occasionally it is comparable [*Cevolani and Bonelli*, 1985; *Thayaparan*, 1997; *Zhao et al.*, 2005]. The amplitude of terdiurnal tide shows day-to-day, seasonal, and interannual variability [*Thayaparan*, 1997; *Beldon et al.*,

2006]. In the present study we found that the terdiurnal tide shows seasonal and interannual variability at equatorial locations. Previous studies from nonequatorial locations have shown that the monthly mean values of this tide are in the range of 2–10 m s^{-1} and that daily values can be as high as 20–30 m s^{-1} [*Smith*, 2000; *Younger et al.*, 2002; *Zhao et al.*, 2005; *Beldon et al.*, 2006]. The monthly mean values of 1–10 m s^{-1} observed in the equatorial region in the present study are comparable to those observed at middle and high latitudes, although the daily values in the present study are only as high as 15 m s^{-1}, less than those recorded at other latitudes.

[26] In a modeling study, *Akmaev* [2001] reported that over the equator, the maximum mean amplitude of the terdiurnal tide to be ~5 m s^{-1} for the zonal component and ~2 m s^{-1} for the meridional component at 94 km. The present observations yield monthly mean values as high as 10 m s^{-1} at 94 km, comparable to values observed at higher latitudes but much higher than modeled values. *Akmaev* [2001] also reported that the zonal amplitude of the terdiurnal tide over the equator is larger than that at the conjugate points used in the present study; the opposite result was obtained for the meridional component. The present observations, in contrast, show that the amplitudes at Pameungpeuk are always smaller than those observed over the equator and at the conjugate point at Tirunelveli. The amplitudes over Tirunelveli, however, are comparable to those over Koto Tabang. Thus, the present observations do not agree with model simulations. However, it is important to note that *Akmaev* [2001] modeled the migrating terdiurnal tide only. The phase difference at the three locations in the present observations shows that the tide may be a mixture of migrating and nonmigrating tides. Discrepancies among various studies may also arise from interannual variability, instrumental bias, or latitudinal differences.

[27] Further, *Batista et al*. [2004] at Cachoeira Paulista (22.7°S, 45°W) showed that the amplitudes of the meridional component of the terdiurnal tide exceed those of the zonal component. Using a meteor radar at Maui (20.75°N, 156.43°W), *Jiang et al*. [2009] showed that the meridional component of the terdiurnal tide is larger than that of the zonal component. *Smith* [2000] studied the latitudinal structure of the terdiurnal tide from satellite observations, revealing that over the equator the zonal component of the tide is larger than the meridional component; at 20°, however, the opposite trend is found. *Akmaev* [2001] reported similar results based on model simulations. The present study shows that in the equatorial regions the two components are comparable, with the zonal amplitude slightly exceeding the meridional amplitude.

[28] The seasonal variation of the terdiurnal tide varies with latitude. If we consider the previous reports on seasonal variation in the terdiurnal tidal amplitude (see introduction) and arrange them with respect to latitude, a clear pattern emerges. At the high-latitude station Esrange (68°N) the maximum amplitude is observed in autumn (September-October) [*Younger et al.*, 2002], observed in winter at Saskatoon (52°N) [*Manson and Meek*, 1986], and observed in winter and early spring at Garchy (47°N), Montpazier (44°N), and London, Canada (43°N) [*Teitelbaum et al.*, 1989; *Thayaparan*, 1997]. For the low-latitude station at Maui (20.75°N), *Jiang et al*. [2009] reported that the meridional component of the terdiurnal tide shows a semiannual variability with peaks near the equinoxes, whereas the zonal component of this tide shows no such seasonal variability. The strongest amplitudes are observed in March, with a secondary peak in October. For the low latitude, Southern Hemisphere station at Cachoeira Paulista (22.7°S, 45°W), *Batista et al*. [2004] reported similar seasonal variations with the meridional component having larger amplitudes in February-March and smaller amplitudes in winter (June-July). Satellite observations of the terdiurnal tide reveal that the maximum amplitudes at midlatitudes are observed during winter and the fall equinox [*Smith*, 2000].

[29] In the present study, we reported seasonal variation in the terdiurnal tide amplitude at three equatorial locations (8.7°N, 0.2°S, and 7.4°S). The conjugate point observations at Tirunelveli and Pameungpeuk show that the maximum amplitudes occur during March-May. Over the equator, however, the maximum amplitudes occur during April-June. This seasonal variation is more pronounced in the zonal wind. The meridional component at Tirunelveli also shows a clear semiannual oscillation, with a secondary peak during September-November.

[30] Figure 7 summarizes the latitudinal variation of maximum amplitudes, based on the present and previous studies. At high latitudes the maximum amplitudes (primary peak) occur in autumn, at midlatitudes they occur in winter, at low latitudes they occur in late winter and early spring, and over the equator they occur in spring and early summer. Thus, the peak amplitude seems to shift in time from autumn to summer as one moves from high latitudes to the equator. At some locations, the tide also shows a semiannual oscillation; thus, a secondary peak is seen ~6 months after the primary peak shown in Figure 7. Future model simulations on the terdiurnal tide should consider this latitudinal variation in maximum amplitude in order to accurately reproduce the global picture of the terdiurnal tide.

4.2. Possible Generation Mechanisms

[31] As far as the generation of terdiurnal tide is concerned, there exist three possibilities as mentioned in the introduction: 1., direct thermal excitation by solar heating; 2., nonlinear interaction between the diurnal and semidiurnal tides; and 3., interaction of the diurnal tide with gravity waves. The results of model simulations indicate that while the direct solar forcing is the dominant mechanism at middle and high latitudes, nonlinear interaction between the diurnal and semidiurnal tides may make a relatively large contribution at low latitudes [*Smith and Ortland*, 2001]. The modeling results reported by *Akmaev* [2001] indicate that the preferential solar excitation of antisymmetric terdiurnal modes, capable of propagating into the MLT combined with an asymmetric atmospheric response, appears to be primarily responsible for the observed seasonal variability. Akmaev's study also shows that the nonlinear interaction of diurnal and semidiurnal tides may make a noticeable in situ contribution to excitation of the terdiurnal tide at 95–100 km, especially during equinox.

[32] The present observations compare well with the Kyushu-GCM model, which takes into account the solar heating of the atmosphere resulting from all the major constituents. The model also solves nonlinear primitive equations, so that nonlinear interactions between tides and various

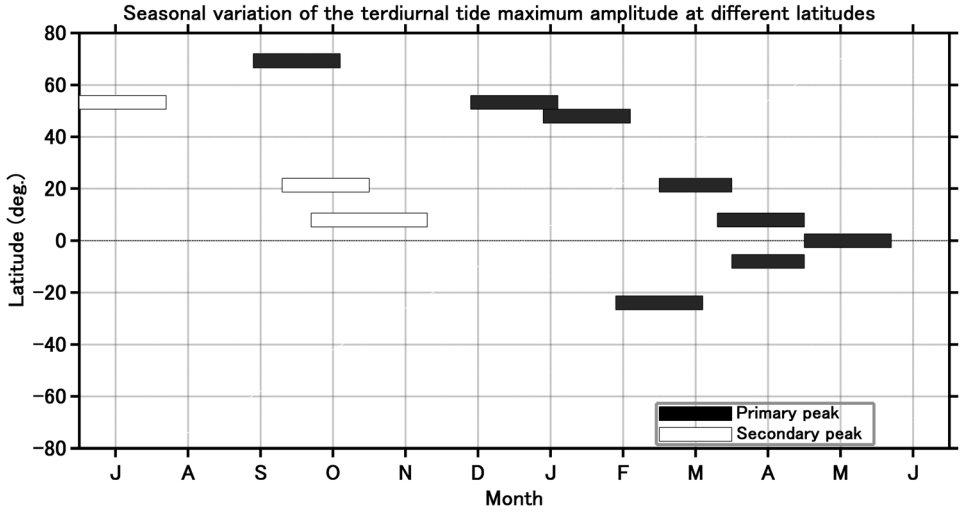

Figure 7. Seasonal and latitudinal variations in the maximum amplitude of the terdiurnal tide, based on the present observations and data from previous reports. Filled blocks represent the primary maximum in terdiurnal tide amplitude; open blocks represent the secondary maximum. Note that the sequence of months shown in Figure 7 starts with July and ends with June.

waves are included. Furthermore, below 95 km height, the effects of unresolved orographic and nonorographic gravity waves are also included. However, the effects of gravity waves are not included using GW parameterization because of the coarse horizontal resolution of the model. Although the observed results agree well with the model values on some occasions, some differences occur, especially during periods with enhanced observed values. Thus, it is necessary to consider the contribution of other sources, such as GW, to the enhancement of the terdiurnal tide amplitude. Before considering the possible contribution of gravity waves, we first examine the possibility that the observed terdiurnal tide is produced by nonlinear interaction between the observed diurnal and semidiurnal tides.

4.2.1. Nonlinear Interaction Between Diurnal and Semidiurnal Tides

[33] Nonlinear interaction between the diurnal and semidiurnal tides could result in the generation of the terdiurnal tide. This possibility has been examined using various approaches. A positive correlation of the diurnal and semidiurnal tidal amplitudes with the terdiurnal tide amplitude has been interpreted to indicate a nonlinear interaction [*Thayaparan*, 1997; *Smith*, 2000]. From a middle-latitude station at London, Canada, *Thayaparan* [1997] reported that for short periods of observations the correlation (cross-correlation coefficient) of the diurnal and semidiurnal tides with that of terdiurnal tide is between 0.4 and 0.75. The correlations shown in their paper were calculated using the entire data set. Based on satellite observations, *Smith* [2000] showed that the terdiurnal tide amplitude correlates weakly (correlation coefficient of 0.2–0.3) with the amplitudes of the diurnal and semidiurnal tides; however, their study included observations from 40°S to 40°N (i.e., an average picture for all latitudes of less than 40°). Furthermore, if the terdiurnal tide is generated by nonlinear interaction between the diurnal and semidiurnal tides, the vertical wavelength relation must also be satisfied [*Thayaparan*, 1997; *Younger et al.*, 2002]. *Thayaparan* [1997] and *Younger et al*. [2002] reported that such a relation holds true in certain periods, thereby supporting the proposal that nonlinear interaction is an excitation mechanism for generation of the terdiurnal tide. At other times, however, this relation does not hold true.

[34] To assess the significance of nonlinear interaction in the present study, we examine the radar observations at Koto Tabang. Figures 8a and 8b shows the monthly mean amplitudes of the terdiurnal, diurnal, and semidiurnal tides for zonal and meridional components, respectively. The three panels in Figures 8a and 8b correspond to heights of 94 km (upper panel), 90 km (middle panel), and 86 km (lower panel). Because Figure 8 was compiled to assess the degree of similarity in the temporal variation of the three tides, the amplitudes are self-normalized for each tide at each altitude. It is apparent that at certain times (e.g., March 2003, October 2003, and February 2007 in the zonal wind at 94 km) the amplitudes are enhanced simultaneously for the terdiurnal, diurnal, and semidiurnal tides; during other periods (e.g., August 2004, September 2006, and March 2007 in the zonal wind at 94 km) the amplitudes are suppressed for all tides simultaneously. However, on some occasions (e.g., April 2003 and September 2007 in the zonal wind at 94 km) the terdiurnal tide amplitude is enhanced without a corresponding enhancement in the diurnal or semidiurnal tidal amplitudes or in both. This is true for both components and at all heights. Thus, we generally observe a one-to-one correspondence between the terdiurnal tide and the diurnal and semidiurnal tides. Accordingly, the present results show that nonlinear interaction occurs most of the time, but not always. Similar variability is observed at the two other locations (data not shown).

[35] To quantify the correlation between the terdiurnal tide and the diurnal and semidiurnal tides, we calculated cross-correlation coefficients for the monthly mean amplitudes, as shown in Figures 9a and 9b for the zonal and

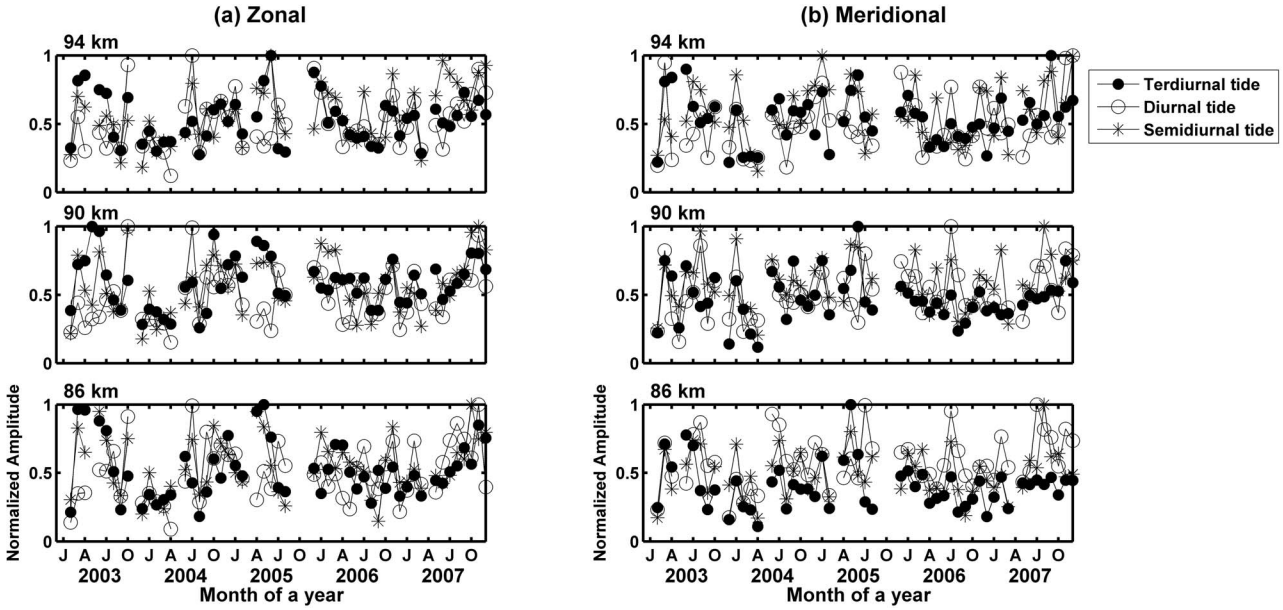

Figure 8. Temporal variations in the monthly mean values of terdiurnal (closed circles), diurnal (open circles), and semidiurnal (asterisks) tides for (a) zonal and (b) meridional winds from January 2003 to December 2007, as observed at Koto Tabang. The three panels in Figures 8a and 8b show data for heights of 94 km (top), 90 km (middle), and 86 km (bottom).

meridional components, respectively. The three panels in each row in Figures 9a and 9b show the correlation of the terdiurnal tide with the semidiurnal tide (first panel), the correlation of the terdiurnal tide with the diurnal tide (second panel), and height profiles of the correlation coefficients (third panel). The overall correlation coefficients between the terdiurnal tide and the semidiurnal tide are 0.86 for the zonal component and 0.79 for the meridional component, while for the terdiurnal and diurnal tides the values are 0.69 and 0.71, respectively. Thus, the correlations are moderately strong, supporting the proposal that nonlinear interaction between the diurnal and semidiurnal tides contributes to the generation of the terdiurnal tide. Furthermore, the vertical wavelength relation, as mentioned above, holds true at certain times but not at others (data not shown). However, it is difficult to derive the correct vertical wavelengths because of the limited height range of observations (compared with tidal vertical wavelengths) and because the observed tide here is a mixture of migrating and nonmigrating tides. Therefore, it is not possible to statistically assess the significance of nonlinear interaction in terms of vertical wavelengths.

[36] *Akmaev* [2001] showed that nonlinear interaction between the diurnal and semidiurnal tides makes an in situ contribution to excitation of the terdiurnal tide, especially during equinoxes. The Kyushu-GCM also includes nonlinear interactions between tides (both migrating and nonmigrating) and interactions with planetary waves, and generally shows good agreement with the observed results. Thus, the present results suggest that the nonlinear interaction of diurnal and semidiurnal tides is important and contributes to enhancement of the terdiurnal tide amplitude. However, it is also important to assess the degree to which the correlation or vertical wavelength relation are indicative of nonlinear interaction between diurnal and semidiurnal tides. This approach is necessary because the amplitudes and phases of the nonlinearly generated terdiurnal tide are highly dependent on small variations in the relative phases between diurnal and semidiurnal tides [*Teitelbaum et al.*, 1989]. Further, a high correlation may also result if a common source is responsible for all waves. Hence, caution is required when making conclusive statements regarding nonlinear interaction as a source in the generation of the terdiurnal tide based on correlation analysis or vertical wavelength relations alone.

4.2.2. Relation Between Terdiurnal Tide Amplitude and Gravity Wave Activity

[37] *Teitelbaum et al*. [1989] encountered difficulties in explaining their wintertime observations (a relatively stable phase and long vertical wavelengths) based solely on solar heating and nonlinear interaction between diurnal and semidiurnal tidal phase structures. Consequently, they suspected a contribution by nonsolar modes and gravity waves with 8 hour periodicity. Using a time-dependant numerical model, *Miyahara and Forbes* [1991] investigated the interaction between gravity waves and the diurnal tide. They showed that GW stresses modified by the diurnal tide induce significant semidiurnal and terdiurnal tides in the MLT region. The amplitude of the resulting terdiurnal tide was 2 m s^{-1} in midlatitude regions. This amplitude is generally smaller than their counterparts generated by direct thermal excitation or nonlinear interaction. However, because of the difficulties with the WKB approximation used in their parameterization, the model interactions were restricted to the extratropics.

[38] The Kyushu-GCM, described in previous sections, considers solar heating by various atmospheric constituents and the nonlinear interactions between tides and various atmospheric waves. Given the deviation between the model

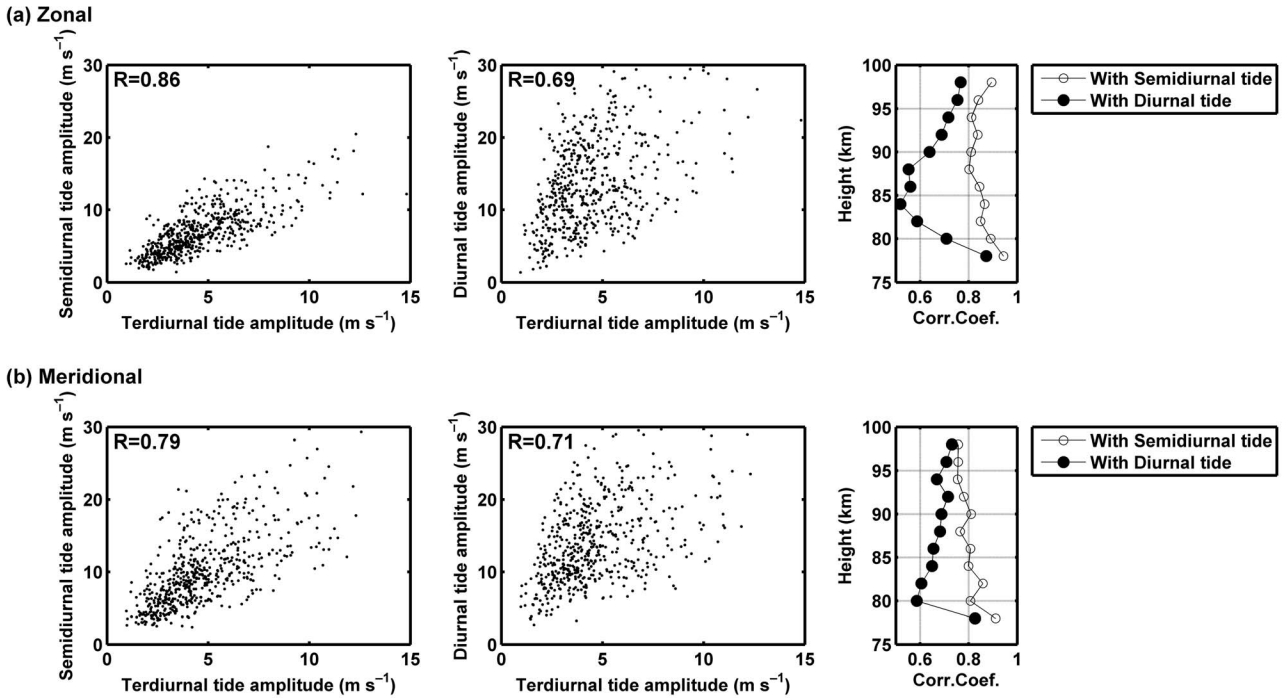

Figure 9. Cross-correlation coefficients between terdiurnal and semidiurnal tides (left-hand panel) and between terdiurnal and diurnal tides (middle panel) for (a) zonal wind and (b) meridional wind. The right-hand panels show height profiles of cross-correlation coefficients between terdiurnal and semidiurnal tides (open circles), and between terdiurnal and diurnal tides (closed circles).

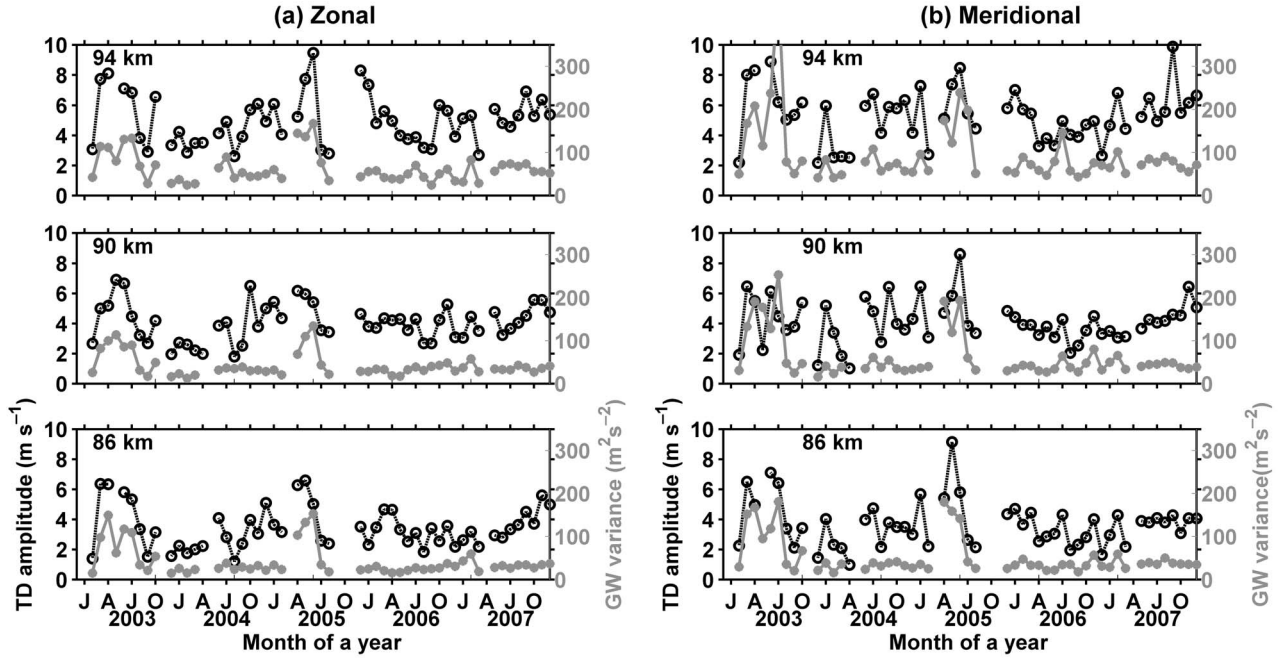

Figure 10. Temporal variation in monthly mean values of terdiurnal tide amplitude (black line with open circles) and gravity wave variance (shaded line with closed circles) for (a) zonal and (b) meridional components. The three panels in each column show data for heights of 94 km (top), 90 km (middle), and 86 km (bottom).

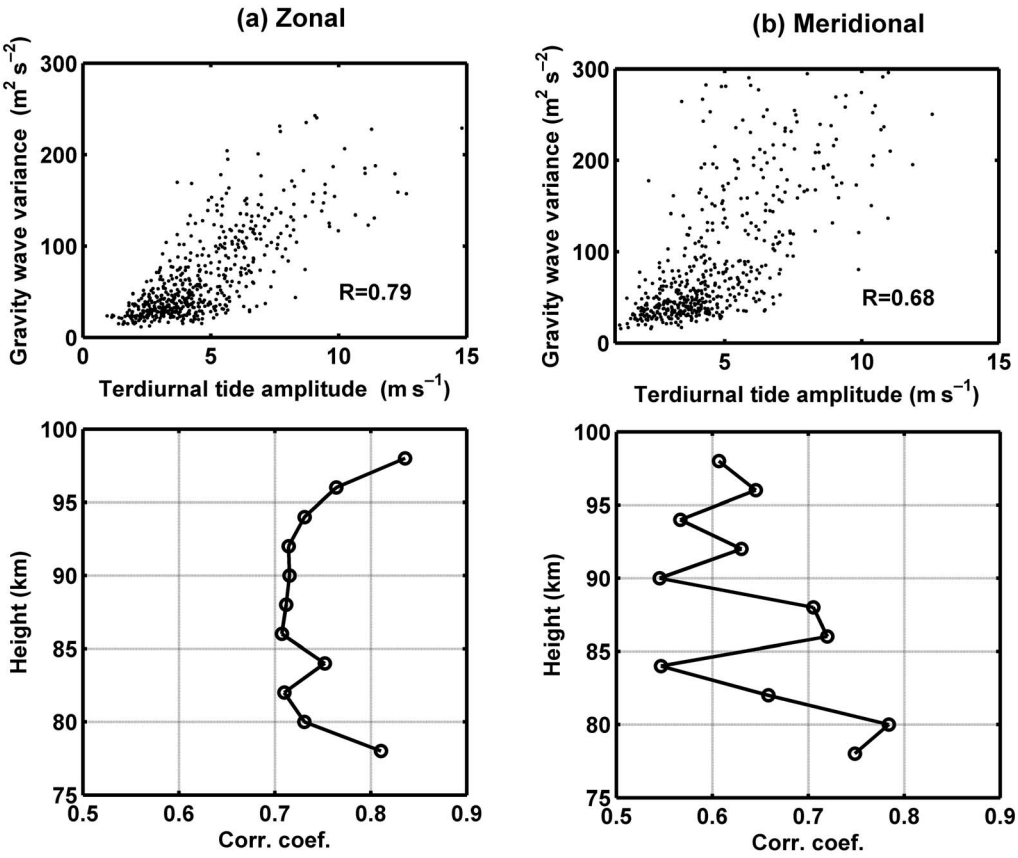

Figure 11. Cross-correlation coefficients between the terdiurnal tide amplitude and gravity wave variance for (a) zonal and (b) meridional winds; the lower panels show height profiles of the cross-correlation coefficients.

results and our observations, it is important to assess the contribution from other sources such as gravity waves.

[39] To explore such a possibility in our observations, we chose GW variance as a proxy for GW activity. The GW variance enhances when there are more GW with modest amplitudes or GW with stronger amplitudes. Figures 10a and 10b shows the monthly mean values of GW variance along with terdiurnal tide amplitude for the zonal and meridional components, respectively. The three panels in each column of Figures 10a and 10b represent observations at 94 km (top), 90 km (middle), and 86 km (bottom). The GW variance is estimated as follows. The mean and tidal components (24, 12, 8, and 6 hour) are removed from the original wind. The residual wind is then subjected to a 2–6 hour band-pass filter. A block of 5 days shifted by 1 day each time is selected to estimate variance. The monthly mean is calculated for such variances and plotted along with the monthly mean of the terdiurnal tide. Figure 10 shows that enhanced amplitude of the terdiurnal tide is associated with corresponding enhancement in gravity wave variance. This is clearly seen during April-June, especially in 2003 and 2005. Furthermore, there exists an increasing trend in both the terdiurnal tide amplitude and GW variance during the period from January 2004 to January 2005. These features are clear at all heights and for both components.

[40] Figures 11a and 11b shows the cross-correlation coefficients between the monthly mean terdiurnal tide amplitudes and GW variance, for the zonal and meridional components, respectively. The overall coefficients are 0.79 for the zonal component and 0.68 for the meridional component. These coefficients vary with height and show an overall decreasing trend for the meridional component. For the zonal component, the coefficient decreases up to 82 km height, is largely constant between this height and 92 km, and increases with a further increase in height. A similar analysis was performed for Tirunelveli and Pameungpeuk (data not shown), revealing that GW activity and terdiurnal tide amplitude show similar variation at Tirunelveli but not at Pameungpeuk. These findings indicate that gravity waves play an important role in the generation of the terdiurnal tide, possibly by interacting with the diurnal tide, and contribute to the observed seasonal variability, at least at Tirunelveli and Koto Tabang. However, it is important to note that a correlation does not necessarily imply cause and effect. It is also possible that gravity waves near 8 hour periodicity are likely to contribute to the observed terdiurnal tide, especially during periods of enhanced GW activity.

[41] The terdiurnal tide appears to be a permanent feature of the equatorial MLT region. Each of the mechanisms mentioned above may play an important role in generating the terdiurnal tide at certain times of the year, and they may also coexist during certain periods. The global occurrence, seasonal and interannual variability, and magnitude of the terdiurnal tide highlight its significance in MLT dynamics;

consequently it would be worthwhile to model this tide using the Global Scale Wave Model (GSWM), along with the diurnal and semidiurnal tides. Furthermore, to obtain a global picture, it would be interesting to study the characteristics and variability of this tide based on midlatitude and high-latitude, ground-based observations in the Southern Hemisphere.

5. Conclusions

[42] We studied the occurrence characteristics and variability of the terdiurnal tide at three equatorial locations: Tirunelveli (8.7°N, 77.8°E), Koto Tabang (0.2°S, 100.3°E), and Pameungpeuk (7.4°S, 107.4°E). Based on the results of this study, we draw the following conclusions regarding the terdiurnal tide: 1., The terdiurnal tide exists as a distinct wave signature at all three equatorial locations, in both zonal and meridional winds; 2., the amplitude of the terdiurnal tide at Pameungpeuk is smaller than that observed at Tirunelveli and Koto Tabang, especially in the zonal wind; 3., the amplitude shows both annual and semiannual variations; 4., the present observations, combined with previous reports, show that the maximum amplitude of the terdiurnal tide shifts from the autumn equinox at high latitudes to winter at midlatitudes, spring at low latitudes, and late spring and early summer at the equator (all seasons are with respect to Northern Hemisphere); 5., a comparison of observations with the Kyushu-GCM shows good agreement with some deviations during the periods of enhanced observed values; 6., the terdiurnal tide correlates well with the diurnal and semidiurnal tides, supporting the proposal that nonlinear interaction between the diurnal and semidiurnal tides is a potential source for generation of the terdiurnal tide; and 7., gravity wave activity and terdiurnal tide show similar temporal variations and are strongly correlated suggesting that gravity waves play a an important role in the generation of the terdiurnal tide especially during April-June over the equator.

[43] **Acknowledgments.** The work of N. Venkateswara Rao was supported by the Japan Society for the Promotion of Science foundation (ID P09232). The Koto Tabang meteor radar and the Pameungpeuk MF radar are operated as a collaborative project between RISH and LAPAN. This study was supported in part by the Japanese Ministry of Education, Culture, Sports, Science and Technology (MEXT) through grants-in-aid for Scientific Research (19403009 and 22253006).

References

Akmaev, R. A. (2001), Seasonal variations of the terdiurnal tide in the mesosphere and lower thermosphere: A model study, *Geophys. Res. Lett.*, *28*, 3817–3820, doi:10.1029/2001GL013002.

Aso, T. (2003), An overview of the terdiurnal tide observed by polar radars and optics, *Adv. Polar Upper Atmos. Res.*, *17*, 167–176.

Batista, P. P., B. R. Clemesha, A. S. Tokumoto, and L. M. Lima (2004), Structure of the mean winds and tides in the meteor region over Cachoeira Paulista, Brazil (22.7°S, 45°W) and its comparison with models, *J. Atmos. Sol. Terr. Phys.*, *66*, 623–636.

Beldon, C. L., H. G. Muller, and N. J. Mitchell (2006), The 8 hour tide in the mesosphere and lower thermosphere over the UK, 1988–2004, *J. Atmos. Sol. Terr. Phys.*, *68*, 655–668.

Cevolani, G. (1987), Tidal activity in the meteor zone over Budrio, Italy, *Int. Counc. Sci. Unions Middle Atmos. Program Handb. MAP*, *25*, 121–137.

Cevolani, G., and P. Bonelli (1985), Tidal activity in the middle atmosphere, *Nuovo Cimento Soc. Ital. Fis. C*, *8*, 461–467, doi:10.1007/BF02582675.

Chapman, S., and R. S. Lindzen (1970), *Atmospheric Tides: Thermal and Gravitational*, D. Reidel, Dordrecht, Neth.

Forbes, J. M., S. E. Palo, X. Zhang, Yu. I. Portnyagin, N. A. Makarov, and E. G. Merzlyakov (1999), Lamb waves in the lower thermosphere: Observational evidence and global consequences, *J. Geophys. Res.*, *104*, 17,107–17,115, doi:10.1029/1999JA900044.

Glass, M., and J. L. Fellous (1975), The eight hourly (terdiurnal) component of atmospheric tides, *Space Res.*, *15*, 191–197.

Gurubaran, S., D. Narayana Rao, G. Ramkumar, T. K. Ramkumar, G. Dutta, and B. V. Krishna Murthy (2008), First results from the CAWSES-India tidal campaign, *Ann. Geophys.*, *26*, 2323–2331.

Jiang, G., J. Xu, and S. J. Franke (2009), The 8 hr tide in the mesosphere and lower thermosphere over Maui (20.75°N, 156.43°W), *Ann. Geophys.*, *27*, 1989–1999.

Manson, A. H., and C. E. Meek (1986), Dynamics of the middle atmosphere at Saskatoon (52°N, 107°W): A spectral study during 1981–1982, *J. Atmos. Terr. Phys.*, *48*, 1039–1055.

Miyahara, S., and J. M. Forbes (1991), Interactions between gravity waves and the diurnal tide in the mesosphere and lower thermosphere, *J. Meteorol. Soc. Jpn.*, *69*, 523–531.

Miyahara, S., Y. Yoshida, and Y. Miyoshi (1993), Dynamic coupling between the lower and upper atmosphere by tides and gravity waves, *J. Atmos. Terr. Phys.*, *55*, 1039–1053.

Miyoshi, Y. (1999), Numerical simulation of the 5 day and 16 day waves in the mesopause region, *Earth Planets Space*, *51*, 763–772.

Miyoshi, Y., and H. Fujiwara (2003), Day-to-day variations of migrating diurnal tide simulated by a GCM from the ground surface to the exobase, *Geophys. Res. Lett.*, *30*(15), 1789, doi:10.1029/2003GL017695.

Pendleton, W. R., Jr., M. J. Taylor, and I. C. Gardner (2000), Terdiurnal oscillations in the OH Meinel rotational temperatures for fall conditions at northern midlatitude sites, *Geophys. Res. Lett.*, *27*, 1799–1802, doi:10.1029/2000GL003744.

Reddi, C. R., and G. Ramkumar (1997), Climatologies of tidal winds in the radio meteor region over Trivandrum (8°N), *J. Atmos. Sol. Terr. Phys.*, *59*, 1757–1777.

Reddi, C. R., K. Rajeev, and R. Geetha (1993), Tidal winds in the radio meteor region over Trivandrum (8.5°N, 77°E), *J. Atmos. Terr. Phys.*, *55*, 1219–1231.

Smith, A. K. (2000), Structure of the terdiurnal tide at 95 km, *Geophys. Res. Lett.*, *27*, 177–180, doi:10.1029/1999GL010843.

Smith, A. K., and D. A. Ortland (2001), Modeling and analysis of the structure and generation of the terdiurnal tide, *J. Atmos. Sci.*, *58*, 3116–3134.

Teitelbaum, H., F. Vial, A. H. Manson, R. Giraldez, and M. Massebeuf (1989), Nonlinear interaction between the diurnal and semidiurnal tides: Terdiurnal and diurnal secondary waves, *J. Atmos. Terr. Phys.*, *51*, 627–634.

Thayaparan, T. (1997), The terdiurnal tide in the mesosphere and lower thermosphere over London, Canada (43°N, 81°W), *J. Geophys, Res.*, *102*, 21,695–21,708.

Tokumoto, A. S., P. P. Batista, and B. R. Clemesha (2007), Terdiurnal tides in the MLT region over Cachoeira Paulista (22.7°S, 45°W), *Rev. Bras. Geofis.*, *25*, 69–78.

Tsuda, T., K. Ohnishi, F. Isoda, T. Nakamura, R. A. Vincent, I. M. Reid, S. W. B. Harijono, T. Sribimawati, A. Nuryanto, and H. Wiryosumarto (1999), Coordinated radar observations of atmospheric diurnal tides in equatorial regions, *Earth Planets Space*, *51*, 579–592.

VanZandt, T. E. (1982), A universal spectrum of buoyancy waves in the atmosphere, *Geophys. Res. Lett.*, *9*, 575–578, doi:10.1029/GL009i005p00575.

Vincent, R. A., S. Kovalam, D. C. Fritts, and J. R. Isler (1998), Long-term MF radar observations of solar tides in the low-latitude mesosphere: Interannual variability and comparisons with GSWM, *J. Geophys. Res.*, *103*, 8667–8683.

Younger, P. T., D. Pancheva, H. R. Middleton, and N. J. Mitchell (2002), The 8 hour tide in the Arctic mesosphere and lower thermosphere, *J. Geophys. Res.*, *107*(A12), 1420, doi:10.1029/2001JA005086.

Zhao, G., L. Liu, B. Ning, W. Wan, and J. Xiong (2005), The terdiurnal tide in the mesosphere and lower thermosphere over Wuhan (30°N, 114°E), *Earth Planets Space*, *57*, 393–398.

H. Fujiwara, Department of Geophysics, Tohoku University, Sendai, JP-980-8578, Japan.

S. Gurubaran, Equatorial Geophysical Research Laboratory, Indian Institute of Geomagnetism, Krishnapuram, Tirunelveli, IN-627 011, India.

Y. Miyoshi, Department of Earth and Planetary Sciences, Kyushu University, 6-10-1 Hakozaki, Higashi-ku, Fukuoka, JP-812-8581, Japan.

T. Tsuda and N. Venkateswara Rao, Research Institute for Sustainable Humanosphere, Kyoto University, Gokasho, Uji City, Kyoto Prefecture, JP-611-0011, Japan. (nvrao@rish.kyoto-u.ac.jp)